High Speed Crystal Growth in Phase-change Recording Materials for Practical Use

Toshiyuki Matsunaga [a], Rie Kojima [b], Noboru Yamada [c], Kouichi Kifune [d] Yoshiki Kubota [e], Sinji Kohara [f]

[a] Device Solutions Center, R&D Division, Panasonic Corporation
3-1-1 Yagumo-Nakamachi, Moriguchi, Osaka 570-8501, Japan
Correspondence e-mail: matsunaga.toshiyuki@jp.panasonic.com

[b] AVC Networks Company, Panasonic Corporation / [c] Department of Materials Science & Engineering, Kyoto University / [d] Faculty of Liberal Arts and Sciences, Osaka Prefecture University / [e] Graduate School of Science, Osaka Prefecture University / [f] Japan Synchrotron Radiation Research Institute/SPring-8

ABSTRACT

Phase change recording is now extensively used for high density non-volatile memories. The typical phase-change materials are GeTe-Sb_2Te_3 pseudo-binary alloys and Sb-Te based multinary alloys with some dopants such as Ag-In-Sb-Te quadruple compounds. These crystals approximately have two kinds of crystalline, metastable and stable phases. The crystals of these metastable phases are very simple and can be approximated by cubic structures; on the other hand, those of stable phases have very complicated long-period layer structures. This structural feature, which is that these materials have cubic-like crystalline phases, is one of major reasons for them to enable such high-speed phase change. The crystal structures of these two phase-change recording materials surprisingly resemble each other; all these crystals consist of 3+3 coordination structures in average irrespective of their phases. In addition, the atomic configurations of these transient crystalline phases of both materials vary with temperature from such simple cubic-like structures to very complicated long-period layer structures through atomic diffusion.

Key words: phase-change memory, GST, AIST, XRD, structural analysis, Rietveld method

1. Overview of structures and their transformations

Phase change recording is now extensively used for high density non-volatile memories [1]. Since 1970s, various materials have been proposed for the purpose, and today we have obtained two superior materials of GeTe-Sb_2Te_3 (GST) [2] and Sb-Te based alloys such as Ag-In-Sb-Te quadruple compounds (AIST) [3]. The crystals of these materials have two, stable and metastable phases; their structures are astonishingly similar to each other. When their amorphous materials are annealed, metastable crystalline structures are first formed; after that, stable phases are built up. The stable phases have long-period stacking structures with cubic close-packed periodicity; on the other hand, the metastable phases show six-layer structures. More precisely, that for GST metastable crystals is an NaCl-type structure; on the other hand, AISTs exhibit A7-type structures. These two kinds of transient structures are, however, very similar to each other, although their structure types are different to each other. It is worth mentioning that all these metastable and stable crystals can be also described as commensurately or incommensurately modulated structures. We can find significant difference between the transformation of the metastable to stable crystalline phase, and that of the amorphous and metastable crystalline phase. It is presumed that the former is caused by atomic diffusion; on the other hand, the latter is originated in interchanges of atomic bonds almost without the atomic diffusion.

2. Structural details of the crystals

Two kinds of chalcogenide compounds, GeTe-Sb_2Te_3 and Sb-Te, have two kinds of crystalline phases, stable and metastable phases. The stable phases have very complicated long period structures; on the other hand, the structures of the metastable phases are very simple and spatially isotropic like amorphous structures.

2-1) Stable crystalline phases

It has been found that in thermal equilibrium, these systems form various intermetallic compounds represented by the chemical formulas $(GeTe)_n(Sb_2Te_3)_m$ and $(Sb_2)_n(Sb_2Te_3)_m$ (n, m: integer), respectively. All these compounds have trigonal structures with $2n + 5m$ cubic close-packed periodicity without exception (more specifically, the residual of $(2n + 5m)/3 = 0$ and $\neq 0$ leads to the space groups, $P\bar{3}m1$ and $R\bar{3}m$, respectively); and they are called homologous compounds because of their similarity in structure. These two kinds of (pseudo-) binary crystals are isostructures to each other when n and m each are respectively the same as those of the other. Their structures are systematically characterized by the stacking of the $(GeTe)_n$ and $(Sb_2Te_3)_m$ or $(Sb_2)_n$ and $(Sb_2Te_3)_m$ blocks along the $\boldsymbol{c}_H$-axes, with very long cell dimensions in the conventional three-dimensional (3-D) structure description [4-13]. More generally and more precisely; it has been assumed that these structures should be described as commensurately or incommensurately modulated four-dimensional (4-D) structures characterized by modulation vectors $\boldsymbol{q} = \gamma \cdot \boldsymbol{c}^*_{\mathrm{sub}}$ in the reciprocal space [14]. As seen in Fig. 1, in the real space, $\boldsymbol{c}_{\mathrm{sub}}$ is the fundamental vector formed by three-layer cubic stacking. In an actual structure modulated by another vector $\boldsymbol{c}_{\mathrm{sub}}/\gamma$ along the $\boldsymbol{c}$-axis, the shifts ($\Delta\boldsymbol{u}$) of the atoms from their equivalent positions ($k\,\boldsymbol{c}_{\mathrm{sub}}; k = \pm1, \pm2, \cdots$) can be written as

$$\Delta\boldsymbol{u}(z) = \Delta\boldsymbol{u}(z + k|\boldsymbol{c}_{\mathrm{sub}}|/\gamma). \qquad (1)$$

This other vector $\boldsymbol{c}_{\mathrm{sub}}/\gamma$ is called modulation vector. We can understand such modulation structures with a notion that the atomic positions with a base frequency are varied by another frequency, and can also regard such a modulated structure as one kind of a distorted structure. When γs are rational numbers, their structures correspond to commensurate structures; otherwise incommensurate structures. For these (pseudo-) binary compounds, we can simply derive γ in terms of x as

$$\gamma = 2 - x/2, \qquad (2)$$

when the chemical formula for these (pseudo-)binary systems are written as $(GeTe)_x(Sb_2Te_3)_{1-x}$, or Sb_xTe_{1-x} [14]. Therefore, only when γs are restricted to (discrete) rational numbers written by $3(n+3m)/(2n+5m)$, they compose commensurate structures. In the GeTe-Sb_2Te_3 pseudo-binary system, several intermetallic compounds exclusively crystallized into commensurately modulated structures, $Ge_3Sb_2Te_6$ (n=3, m=1; 11R)[10], $Ge_2Sb_2Te_5$ (n=2, m=1; 9P)[9], $Ge_1Sb_2Te_4$ (n=1, m=1; 7R)[8], $Ge_1Sb_4Te_7$ (n=1, m=2; 12P)[12], and $Ge_1Sb_6Te_{10}$ (n=1, m=3; 17R)[13], have been found up to now to our knowledge; while it has been presumed that the Sb-Te binary system contains not only such intermetallic compounds as the GST materials but also a (wide) composition region seamlessly filled with incommensurate Sb_xTe_{1-x} compounds around Sb:Te=1:1. In these structures, all the constituent atoms have 3+3 coordination atoms, which form distorted octahedral coordination same as in the metastable structures. The central atom is more strongly bonded with the shorter three atoms than the other three.

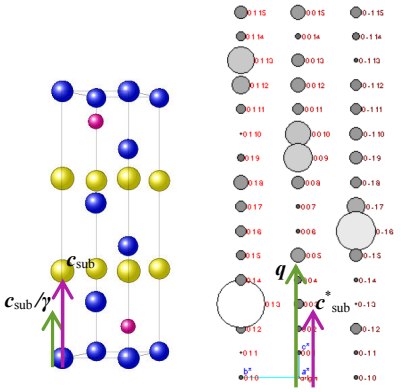

Fig. 1. The crystal structure of $Ge_2Sb_2Te_5$ and its diffraction pattern. The structure is shown in perspective, in which Ge, Sb, and Te are indicated by purple, yellow and blue, respectively. The $0k\ell$ diffraction plane is depicted in a square range of $-1 \le k \le 1$ and $0 \le \ell \le 15$. The diameters of the reciprocal points in the pattern are in proportion to the absolute values of their structure factors $F(0k\ell)$. The atomic layers along the c_H-axis are arranged by two kinds of vectors in this structure: one is the fundamental reciprocal vector formed by three-layer cubic stacking and the other is a modulation vector expressed by $\boldsymbol{q} = \gamma \cdot \boldsymbol{c}^*_{\mathrm{sub}}$. The former vector gives fundamental reflections; on the other hand, the latter produces superstructure reflections on the diffraction patterns. The γ value of this crystal is a rational number 5/3; which means that it has a commensurate structure. In actual $Ge_2Sb_2Te_5$ crystals, it is presumed that the Ge and Sb sites are partially substituted by Sb and Ge atoms, respectively [9].

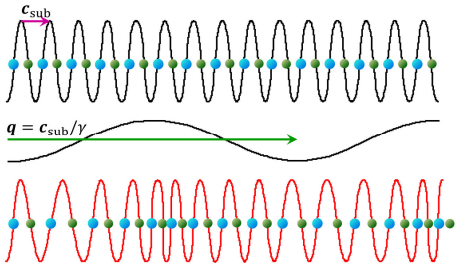

Fig. 2. Schematic view of frequency modulation. The frequency of the carrier signal (top) varies as the voltage of the modulating signal (middle) changes to the radio frequency signal (bottom). The atoms seen in this figure form a two-layer structure. They shift from the equivalent positions owing to the frequency modulation.

2-2) Metastable crystalline phases

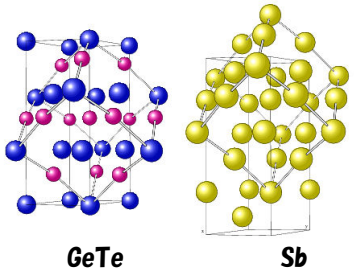

Fig. 3. The structures of the GeTe low-temperature phase ($R3m$) and Sb ($R\bar{3}m$) shown in the hexagonal (thin lines) unit cells. The NaCl-type structure of the high-temperature phase for GeTe drawn with thick lines is deformed by the phase transition to the low-temperature phase. (Pseudo-) cubic cell is depicted with thick lines as well also in the Sb structure model. This large cubic cell is composed of eight small, pseudo simple cubic cells. As seen in these drawings, both crystals are six-layer structures, any constituent atom has six (3+3) coordination atoms (three atoms at upper layer + three atoms at lower layer).

Just after the phase transformation from the amorphous phase, which corresponds to deleting recorded marks in optical disks, GST and AIST amorphous compounds both crystallize into six-layer homologous structures. The formers are B1-type (NaCl) structures; on the other hand, the latters are A7-type (α-As) structures. The A7-type crystals hold 3+3 coordination structures as well as other homologous crystals mentioned above. The octahedra formed by these coordination atoms are oriented along the *c*-axis directions. Recently, it has been found that GeTe also maintains 3+3 coordination structure even in its high-temperature cubic phase; however, the octahedra of this crystal are randomly distributed different from the case of AIST [18] (Not only in this binary compound but also in GST pseudo-binary cubic compounds; we believe that such coordination structures remain even in their cubic phases). These two structures are naturally very similar to each other as seen in Fig. 3, because they are ones of homologous structures in common. If Ge and Te atoms are randomly located at any atomic sites of the GeTe crystal, its structure coincides with that of Sb. These structures are the simplest (γ=3/2) of all the homologous structures, and they are spatially isotropic, which can be well approximated by cubic structures. We have been asserting that the materials that can take such simple and spatially isotropic structures just after the recrystallization are suitable for high-speed phase-change recording materials; it is presumed that such a structural property is one of the essential features for them because topological resemblance is required for reduction of atomic switch lengths through the phase change.

2-3) Structural transformations in the crystalline phases

As mentioned in the introduction, NaCl-type GST (metastable) crystals transform to the stable trigonal structures by giving sufficient heat treatments. These structural transformations are first-order phase transition phenomena. The former crystals suddenly change to the latters when raising the temperature. These transition temperatures have been examined by the differential scanning calorimetry [2]. For instance, metastable $Ge_2Sb_2Te_5$ maintains its NaCl-type structure up to 230 ºC; above this transition temperature, the crystal abruptly changes to 9-layer trigonal structure (see Fig. 1) with showing an exothermic peak. The γ values characterizing these structures are 3/2 and 5/3, respectively; the above means that γ discretely changes from the former to the latter at its specific transition temperature. In the cases of $Ge_1Sb_2Te_4$, it falls into 21-layer structure (γ=12/7) at 210 ºC. The metastable structures transform to the stable structures through atomic diffusion as shown in Fig.4. On the other hand, different from these GST compounds, the atomic rearrangements in Sb-Te crystals show second order-like phase transformations.

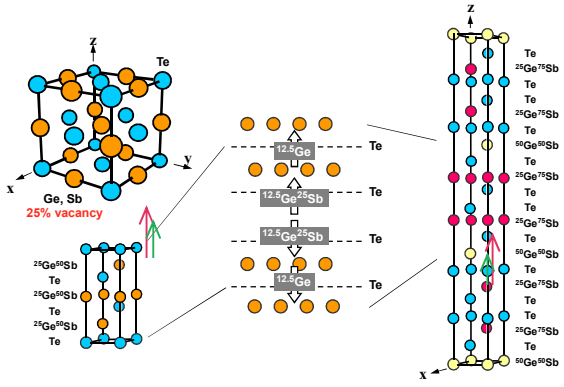

Fig. 4. The schematic drawing of the atomic diffusion in the metastable $GeSb_2Te_4$ crystal. The diffusion causes the structure transition from the metastable phase (on the left) to the stable phase (on the right). The Ge/Sb layer in the metastable phase includes vacancies up to 25 at.%. It is logical to assume that the atomic diffusion of Ge and Sb towards the vacancies, as shown in this figure, generates the structure transformation from the former to the latter.

Sb-Te materials are used in practice as phase-change recording materials by doping third and/or fourth elements such as Ag and/or In to improve the endurance of the amorphous phase and raise the transition temperature to the crystalline phase. The diffraction patterns in a heating process obtained for the sputtered AIST ($Ag_{3.4}In_{3.7}Sb_{76.4}Te_{16.5}$) amorphous film are shown in Fig. 5 [15]. The amorphous phase transformed into an A7-type crystalline single phase, as seen in this graph, at (around) 416 K. This six-layer crystalline phase is kept up to around

545 K; however, phase separation written by the following equation takes place above this temperature.

$$Ag_{3.4}In_{3.7}Sb_{76.4}Te_{16.5} \rightarrow Ag_{3.4}In_{3.4}Te_{6.8} + In_{0.3}Sb_{76.4}Te_{9.7}. \quad (3)$$

The first decomposition product has a $CuFeS_2$-type structure, which was tightly held up to the melting temperature around 870 K. The second product, which can virtually be regarded as an Sb-Te binary compound written as $Sb_{89}Te_{11}$ (when expressed as a percentage), gradually changes its atomic arrangement with increasing temperature until obtaining the final stable crystal structure. The atomic configuration determined for the latter is shown in Fig. 6 as an approximated 3-D structure with γ = 45/29. As seen in Fig. 7, γ maintained a constant value of 1.5 up to a temperature of around 591 K, at which $AgInTe_2$ ($CuFeS_2$-type structure) came out. However, above this temperature, γ continuously grew larger with increasing temperature and reached a value of around 1.55 at high temperatures near the melting point (~870K) of $Sb_{89}Te_{11}$. This γ value corresponded well with the value of 1.5565 expected from the composition of $Sb_{88.7}Te_{11.3}$ [see Eq. (2)].

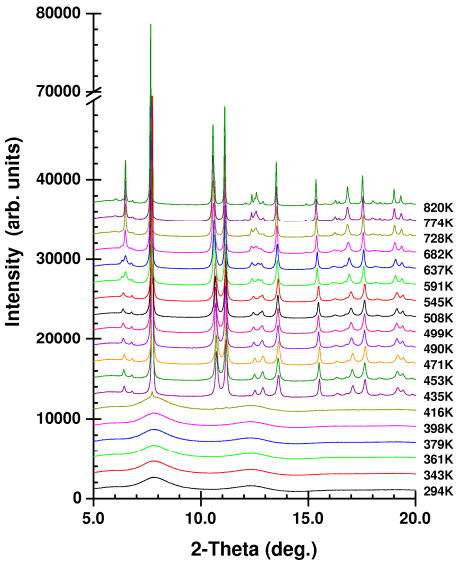

Fig. 5. Temperature dependence of the X-ray powder diffraction profiles for a sputtered $Ag_{3.4}In_{3.7}Sb_{76.4}Te_{16.5}$ amorphous film in a heating process. The amorphous halo patterns are observed at low temperatures from 295 K to 416 K; however at around 416 K, the Bragg peaks of A7-type structure appear in the halo pattern. As temperature is raised further, the A7-type single phase separates into two phases, $AgInTe_2$ and an Sb-Te binary compound, at around 591 K. At lower 2θ angles than 5º, Bragg peaks were hardly observed at any measurement temperatures.

As has so far been shown, the structural transformations with temperature in the two materials are notably different from each other. In the GST pseudo-binary materials, γ abruptly changes with temperature at first-order phase transition; on the other hand, in the Sb-Te binary materials, it continuously varies. The latter variation behaves like a second-order phase transition phenomenon. As for materials with Ge atoms, on the other hand, it is conceivable that such obvious first-order phase transitions observed in these materials will probably result from simultaneous breaking of sp^3-electronic configurations of Ge atoms at the specific temperatures.

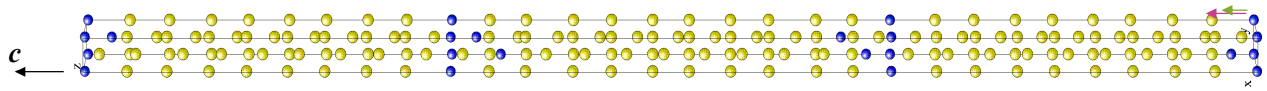

Fig. 6. Structural model of $Sb_{26}Te_3$ (820 K), which is approximated by 3D commensurately modulated structure. The atomic positions of Sb and Te are shown by yellow and blue, respectively. The light purple and chartreuse green inserted in the figure respectively show $\boldsymbol{c}_{sub}$ and $\boldsymbol{c}_{sub}/\gamma$ which characterize this (long period) modulated structure.

3. Structural details of the amorphous phases

In GST amorphous materials, three constituent atoms are strongly connected with a few specific neighboring atoms. Coordination numbers for three constituent atoms approximately follow the 8-*N* rule, different from those of the crystalline phase; for instance, those of a-GST225 are ca 4, 3, and 2.5 around Ge, Sb, and Te atoms respectively (only for Te atoms, about half of them have two coordination atoms and the other half three). The bond lengths are also shorter than in the crystalline phase. These bonding schemes show the characteristics of covalent bonds often observed in chalcogenide amorphous materials. The atomic configuration is maintained almost unchanged up to the transition temperature to the crystalline phase [16], [17]. It has been considered that such a strong covalent bonding nature gives these amorphous materials sufficient endurance, namely, long-term data preservation. In these GST amorphous materials, if three kinds of atoms

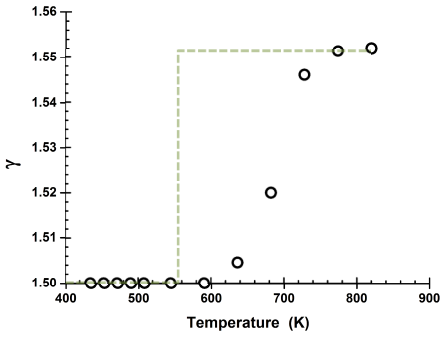

Fig. 7. Temperature dependences of modulation period (O) obtained from 4-D structural analyses for $Sb_{89}Te_{11}$. That for corresponding GST material (x=0.89) is, on the other hand, expected to vary stepwise with temperature as shown by dotted line [2].

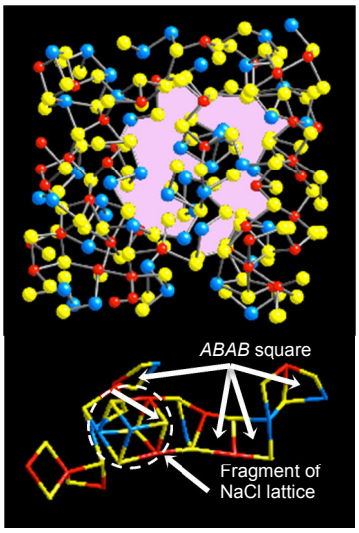

Fig. 8. The amorphous structure (section of 460-atom) solved by a DF-MD method model of a-GST (24 Å × 24 Å × 12 Å) [*]. Ge, red; Sb, blue; Te, yellow; large cavity, pink. A large cavity is present among the atomic arrangement in this structure. Enlarged configuration shows that a-GST has many structural units (ABAB-squares) with alternating Te and Ge (or Sb) atoms. We can observe even a fragment of NaCl lattice.

connect with each other with equal probability, six kinds of atomic pairs should be found at the ratio provided by a random covalent network model. However, GST amorphous materials comprise a far larger number of Ge-Te and Sb-Te atomic pairs than the mean values given by a random covalent network model. This is very interesting because the crystalline phase is formed only by these two pairs. In a-GST225, 40% of the rings are fourfold or six-fold and a considerable amount of the relict $GeTe_4$ tetrahedra and $SbTe_3$ pyramids whose bond angles are distributed around 90º as same as those of the crystalline phase [18], [19]; we can find even NaCl-type crystalline fragments themselves in the amorphous atomic network as seen in Fig. 8. These fragments are innumerably embedded in the amorphous atomic network; then, once sufficient heat energy is supplied to the amorphous material, those crystalline fragments act as first nuclei to crystallize their surroundings all at once.

It was revealed in AIST materials that both a-AIST (left panel) and c-AIST (right panel) assembled (distorted) 3 + 3 octahedra into their structures as shown in Fig. 9. In the amorphous state, interatomic distance between the central atom and three shorter coordination atoms is considerably shorter than in the crystalline state; they are connected to each other by a stronger covalent force than those in the crystal to form isolated molecule by themselves. From a topological point of view, one coordination polyhedron (in this case, an octahedron) composes two tetrahedra; of the two, the one formed by shorter bonds is a basic molecular unit in the amorphous structure. These molecules are weakly connected by vertices or edges; a spatially periodic arrangement is not required of them. For this reason, the orientation vectors made by green arrows are randomly oriented as seen in the left bottom panel of Fig. 9. However, once sufficient heat energy is given to the amorphous material, it causes interchange of one bond in a 3+3 coordination octahedron to rearrange, parallel neighboring two vectors. This rearrangement swiftly propagates from neighbor to neighbor forming the crystalline preferred orientation. This amorphous material contains few crystalline embryos (atomic rings or clusters) as observed in amorphous GST; then crystal growth is much more dominant in the structural transformation from the amorphous to the crystalline phase.

4. basic structure maintained during whole phase transformation

The atomic configuration in the AIST amorphous material, which has already been revealed by Matsunaga *et al*. [20], is heavily disordered, and has a spatially isotropic symmetry. However, it has also been revealed that it serves 3+3 coordination structures even in such a disordered atomic arrangement, as well as that of the crystalline phase: that is, the coordination structures of both phases are very alike, i.e., they have very similar local atomic arrangements (it is well known that an A7-type crystal has a 3+3 coordination structure [21], [22]). This is one of major reasons that this material achieves a sufficiently high phase-change speed by locally minimal bond interchanges. As for the dopants such as Ag or In, it has been presumed that the presence of these atoms, separately or together, serves to raise the crystallization temperature of the amorphous phase to obtain a sufficient endurance for long-term data preservation. As well as the AIST crystal, it has been

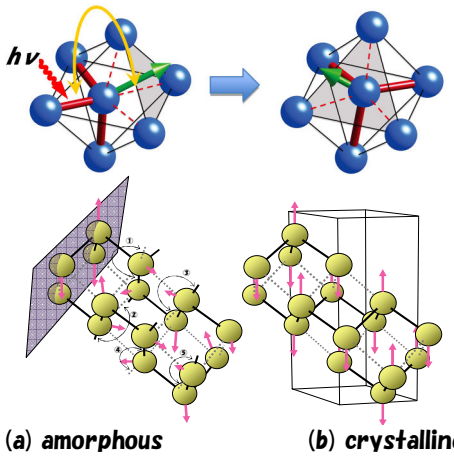

Fig. 9. The central atom with three short (red) and three long (dashed) bonds crosses the center of the distorted octahedron, interchanging a short and a long bond. Green: resultant vector of short bonds. The bonding electrons are excited by laser light ($h\nu$) to cause an interchange of bonding electrons, for example, between the two bonds pointed by the yellow arch, which moves the atoms in the amorphous phase to form locally crystalline atomic configurations; as shown in the lower panels, the local crystalline atomic networks finally form resonant bonding between periodic short and long bonds, which leads to the crystalline A7 network. The shade plane shows a domain wall between crystalline phase and amorphous phase.

revealed that GeTe or GeTe-rich GeTe-Sb_2Te_3 NaCl-type (metastable) crystals also have 3 + 3 coordination structure even in its high-temperature cubic phase [23], and that the three kinds of constituent atoms of these amorphous materials have the coordination numbers of approximately four for Ge, three for Sb, and two or three coordination atoms for Te, fairly well satisfying the 8-N formation of Mott's rule [24]. Then, also in these amorphous materials, the average coordination number corresponds to three. These amorphous materials intrinsically contain an obvious number of crystal-like fragments in their atomic configurations [25], [26]. It is then very likely that, once sufficient energy is given to them by laser irradiation or ohmic heating, crystallization starts from these crystalline embryos all together; and whole amorphous mark are instantaneously crystallized by slight atomic shifts with bond interchanges around the embryos in the same manner of the crystal growth process revealed in AIST.

5. Summary: Physics for high-speed phase change revealed by the structural analysis

In the amorphous phases of the chalcogenide phase-change materials, the atoms are connected by relatively strong covalent bonds; the bonding electrons are localized between them. These atoms locally cohere to form molecules in the system. The energy of the whole system and the configurational entropy are higher than those of the crystalline phases. To cause the transformation from the amorphous to crystalline phase, activation energies are required beyond the thresholds. In other words, sufficient energy is given to the system; the amorphous state is excited, and the localized bonding electrons are used as resonance bondings in the crystalline state. As the results of the phase transition, the free energy of the system decreases. Fortunately, these chalcogenide materials are generally susceptible to visible lights; because their band gaps are sufficiently narrow not only for the crystalline states but also for the amorphous states, and they contain high-density electrons just below the Fermi energies. The narrow-band gap means that bond interchange from covalent bond to resonance bond can easily take place by the incident photons and thermal phonons. In other words, these materials can be instantaneously heated up to the temperatures to cause rapid phase changes to their crystalline phases by laser irradiation. Furthermore, the thermal conductivities of these chalcogenide compounds are surprisingly low even in their crystalline phases, which means that local area of them can be quickly heated up by less energy. Both compounds crystallize to very long-period layer structures in the thermal equilibrium; however, by a happy chance, they have simple cubic or cubic-like structures in common. In addition, their atomic configurations resemble well those of their amorphous phases. This structural feature for these materials enables high-speed phase change from the amorphous to crystalline phase. The amorphous structures can be changed simply by bond interchanges, without atomic diffusion.

REFERENCES

[1] Wuttig, M. & Yamada, N. (2007). *Nat. Mater*. **6**, 824.

[2] Yamada, N., Ohno, E., Nishiuchi, K., Akahira, N. & Takao, M. (1991). *J. Appl. Phys*. **69**(5), 1, 2849

[3] Iwasaki, H., Ide, Y., Harigaya, M., Kageyama, Y. & Fujimura, I. (1992). *Jpn. J. Appl. Phys*. **31**, 461.

[4] Karpinsky, O. G., Shelimova, L. E., Kretova, M. A. & Fleurial, J. –P. (1998). *J. Alloys Compd*. **268**, 112

[5] Shelimova, L. E., Karpinskii, O. G., Zemskov, V. S., & Konstantinov, P. P. (2000) *Inorg. Mater*. **36** (3), 235.

[6] Shelimova, L. E., Karpinskii, O. G., Konstantinov, P. P., Kretova, M. A., Avilov, E. S., & Zemskov, V. S. (2001). *Inorg. Mater*. **37**(4), 342.

[7] Poudeu, P. F. P. & Kanatzidis, M. G. (2005) *Chem. Commun*. 2672.

[8] Matsunaga, T. & Yamada, N. (2004). *Phys. Rev*. B **69**(10), 104111.

[9] Matsunaga, T. & Yamada, N. Kubota, Y. (2004). *Acta Cryst*. B **60**, 685.

[10] Matsunaga, T., Kojima, R., Yamada, N., Kifune, K., Kubota, Y. & Takata, M. (2007). *Appl. Phys. Lett*. **90**, 161919.

[11] Matsunaga, T., Kojima, R., Yamada, N., Kifune, K., Kubota, Y. & Takata, M. (2007). *Acta Cryst*. B**63**, 346.

[12] Matsunaga, T., Kojima, R., Yamada, N., Kifune, K., Kubota, Y. & Takata, M. (2008). *Chem. Mater*. **20**(18), 5750.

[13] Matsunaga, T., Kojima, R., Yamada, N., Fujita, T., Kifune, K., Kubota, Y. & Takata, M. (2010). *Acta Cryst*. B**66**, 407.

[14] Lind, H. & Lidin, S. (2003). *Solid State Sci*. 5, 47.

[15] Matsunaga, T., Kojima, R., Yamada, N., Kubota, & Kifune, K.. (2012). *Acta Cryst*. B**68** (approved for publication).

[16] T. Matsunaga, R. Kojima, N. Yamada, and M. Takata: *Europian¥Phase Change and Ovonics Symposium 2008* (2008).

[17] T. Matsunaga, N. Yamada, R. Kojima, S. Shamoto, M. Sato, H. Tanida, T. Uruga, S. Kohara, M. Takata, P. Zalden, G. Bruns, I. Sergueev, H. C. Wille, R. P. Hermann, M. Wuttig: *Adv. Funct. Mater*. **21**, 12, 2232 (2011).

[18] S. Kohara, K. Kato, S. Kimura, H. Tanaka, T. Usuki, K. Suzuya, H. Tanaka, Y. Moritomo, T. Matsunaga, N. Yamada, Y. Tanaka, H. Suematsu, and M. Takata, *Appl. Phys. Lett*. **89**, 201910 (2006).

[19] J. Akola, R. O. Jones, S. Kohara, S. Kimura, K. Kobayashi, M. Takata, T. Matsunaga, R. Kojima, and N. Yamada: *Phys. Rev. B* **80**, 020201 (2009).

[20] Matsunaga, T., Akola, J., Kohara, S., Honma, T., Kobayashi, K., Ikenaga, E., Jones, R. O., Yamada, N. Takata, M. & Kojima, R. *Nat. Mater*. (2011), **10**, 129.

[21] Clark, G. L. *Applied X-Rays* (McGraw-Hill Book Company, Inc., 1955).

[22] Hoffmann, R. *Solid and Surface* (VCH, New York, 1988).

[23] Matsunaga, T., Fons, P., Kolobov, A. V., Tominaga, J. & Yamada, N. (2011). *Appl. Phys. Lett*. **99**, 231907, 1-3

[24] Mott, N. F. (1969). *Philos. Mag.* B **19**, 835

[25] Kohara, S., Kato, K., Usuki, T., Suzuya, K., Tanaka, H., Tanaka, Y., Kimura, S., Tanaka, H., Moritomo, Y., Matsunaga, T., Yamada, N., Suematsu, H. & Takata, M. (2006). *Appl. Phys. Lett*. **89**

[26] Ohara, K., Temleitner, L., Sugimoto, K., Kohara, S., Matsunaga, T., Pusztai, L., Itou, M., Ohsumi, H., Kojima, R., Yamada, N., Usuki, T., Fujiwara, A. & Takata, M. (2012). *Adv. Funct. Matter*. **22**, 2251